GEOPHYSICAL RESEARCH LETTERS, VOL. 35, L02613, doi:10.1029/2007GL032580, 2008

A new model for Double Diffusion + Turbulence

V. M. Canuto,[1,2] Y. Cheng,[1,3] and A. M. Howard[1,4]

Received 5 November 2007; revised 26 November 2007; accepted 6 December 2007; published 29 January 2008.

[1] Available models of Double Diffusion (DD) processes (Salt Fingers, SF and Diffusive Convection, DC) are primarily based on laboratory experiments that do not include turbulence which is however always present in the ocean. A reliable DD model for use in OGCMs (ocean global circulation models) is therefore still lacking and a true assessment of the role of oceanic DD is yet to be made. Here, we derive and validate a new model for *DD + Turbulence* using a second-order closure model which differs significantly from previous ones in that the ratios of the correlation time scales to the dissipation time scales, constant in previous models, now depend on Ri and R_ρ, the key new feature needed to reproduce both laboratory (no shear) and oceanic (with shear) data. The model can therefore be used in OGCMs. The full mixing model includes mixed layer, internal gravity waves, DD and tides.
Citation: Canuto, V. M., Y. Cheng, and A. M. Howard (2008), A new model for Double Diffusion + Turbulence, *Geophys. Res. Lett.*, *35*, L02613, doi:10.1029/2007GL032580.

1. Introduction

[2] Maps by D. E. Kelley (personal communication, 2007) of the density ratio $R_\rho = (\alpha_s \partial S/\partial z)(\alpha_T \partial T/\partial z)^{-1}$ (T and S are mean temperature and salinity fields and $\alpha_{T,S}$ are the thermal expansion and haline contraction coefficients) show the ocean's regions that are prone to DD instabilities [*Ruddick and Gargett*, 2003]. From those maps one observes that the likelihood of SF is higher in the Atlantic than in most of the Pacific and that DC may play a significant role in the Arctic and in the Southern Ocean, a point discussed by *Kelley et al.* [2003] who concluded that DC "could be of major importance to the properties of the global ocean". DC is more likely in high-latitude precipitation zones [*Schmitt*, 1994] and *Muench et al.* [1990] also found it over much of the Weddell Sea. Overall, in the circumpolar current, both SF and DC may be important. These high latitude regions are of dynamical interest since numerical simulations [*Hasumi and Suginohara*, 1999; *Webb and Suginohara*, 2001] show that a sizeable upwelling of the thermohaline circulation occurs in those regions, in contrast to the traditional view of a uniform upwelling throughout the whole ocean. Since thus far most DD models have been based on laboratory data [see *Kunze*, 2003; *Schmitt*, 1994, 2003; *Kelley et al.*, 2003], they do not represent the true oceanic environment where there is always a turbulent background [the latter can be represented by a Richardson number $Ri = N^2/\Sigma^2$, where N is the Brunt-Vaisala frequency ($N^2 = \partial\overline{b}/\partial z$, $b = -g\rho/\rho_0$ is the buoyancy); Σ is the mean shear ($\Sigma^2 = (\partial U/\partial z)^2 + (\partial V/\partial z)^2$ where U, V are the horizontal mean velocity components)]. Models for DD + Turbulence for arbitrary Ri and R_ρ, have been proposed [*Walsh and Ruddick*, 2000; *Inoue et al.*, 2007] but the presence of unknown parameters precludes their use in OGCMs. *Smyth and Kimura* [2007] employed a linear stability analysis to study DD + Shear but the heat mixing efficiency Γ_h vs. R_ρ was opposite to that of the data (see section 6).

[3] In this paper we present a new model for DD + Turbulence valid for arbitrary Ri, R_ρ and test it against laboratory data (R_ρ, very large Ri) and oceanic data (large range of values of Ri and R_ρ). The data are γ (heat to salt flux ratio) for SF, R_F (salt to heat flux ratio) for DC and Γ_h (heat mixing efficiency) for SF:

$$\gamma(\mathrm{Ri}, R_\rho), R_F(\mathrm{Ri}, R_\rho), \Gamma_h(\mathrm{Ri}, R_\rho) \tag{1}$$

Specifically, $\gamma(\mathrm{Ri}, R_\rho)$ in the $\mathrm{Ri} \gg 1$ limit is taken from *St. Laurent and Schmitt* [1999], *Kunze* [2003] and *Schmitt* [2003], $R_F(\mathrm{Ri}, R_\rho)$ is taken for $\mathrm{Ri} \gg 1$ from *Kelley* [1990] and $\Gamma_h(\mathrm{Ri}, R_\rho)$ is taken from *St. Laurent and Schmitt* [1999]. Since the model reproduces the functions in equation (1) reasonably well, it can be used in OGCMs which need heat and salt diffusivities $K_{h,s}$ that depend on the variables (1).

2. Heat and Salt Diffusivities

[4] Though we are primarily interested in heat and salt fluxes, their dynamic equations depend on other second-order moments and one must therefore consider $\overline{u_i w}$, $\overline{w\theta}$, $\overline{ws}$, $\overline{\theta^2}$, $\overline{s^2}$ and $\overline{\theta s}$ representing momentum, heat and salt fluxes, temperature and salinity variances and temperature-salinity correlation whose dynamic equations were presented in equations (5)–(11) of *Canuto et al.* [2002] (hereinafter referred to as C2). In the local and stationary case, such equations can be solved analytically with the following results:

$$\overline{u_i w} = -K_m \frac{\partial U_i}{\partial z}, \ \overline{w\theta} = -K_h \frac{\partial T}{\partial z}, \overline{ws} = -K_s \frac{\partial S}{\partial z}, \quad \overline{wb} = -K_\rho N^2 \tag{2a}$$

$$K_\alpha = \Gamma_\alpha \frac{\varepsilon}{N^2}, \ \Gamma_\alpha = \frac{1}{2}(\tau N)^2 S_\alpha, \Gamma_\rho = \Gamma_h\left(1-\gamma^{-1}\right)\left(1-R_\rho\right)^{-1} \tag{2b}$$

[1]NASA Goddard Institute for Space Studies, New York, New York, USA.
[2]Department of Applied Physics and Applied Mathematics, Columbia University, New York, New York, USA.
[3]Center for Climate Systems Research, Columbia University, New York, New York, USA.
[4]Department of Earth, Atmospheric, and Planetary Sciences, Massachusetts Institute of Technology, Cambridge, Massachusetts, USA.

0094-8276/08/2007GL032580$05.00

where i = 1, 2 (α stands for momentum, heat, salt and density); $\tau = 2K/\varepsilon$ is the dynamical time scale, K is turbulent kinetic energy and ε its rate of dissipation. The form of the dimensionless structure functions $S_\alpha(Ri, R_\rho)$ is given by equations (13a)–(15) of C2. Here, we present an alternative form for $S_{h,s}$ in terms of the ratio $\overline{w^2}/K$:

$$\begin{aligned} S_h &= A_h\left(\overline{w^2}/K\right), \\ S_s &= A_s\left(\overline{w^2}/K\right), \\ \frac{\overline{w^2}}{K} &= \frac{2}{3} - \frac{4}{15}\left(\frac{3}{5}\frac{\Gamma_m}{Ri} + \Gamma_\rho\right) \end{aligned} \tag{2c}$$

$$\begin{aligned} A_h &= \pi_4\left[1 + px + \pi_2\pi_4 x\left(1 - \gamma^{-1}\right)\right]^{-1}, \\ A_s &= \pi_1\left[1 + qx + x\pi_1\pi_2 R_\rho(\gamma - 1)\right]^{-1} \end{aligned} \tag{2d}$$

where γ is the heat to salt flux ratio given by:

$$\gamma = \frac{\alpha_T\overline{w\theta}}{\alpha_S\overline{ws}} = \frac{K_h}{K_s R_\rho} = \frac{1}{R_\rho}\frac{\pi_4}{\pi_1}\frac{1 + qx}{1 + px}$$

where

$$\begin{aligned} &q = \pi_1\pi_2\left(1 + R_\rho\right) - \pi_1\pi_3 R_\rho, p = \pi_4\pi_5 - \pi_2\pi_4\left(1 + R_\rho\right), \\ &x = (\tau N)^2\left(1 - R_\rho\right)^{-1} \end{aligned} \tag{2e}$$

[5] The π's represent relaxation-dissipation time scales of the different second-order moments and are discussed in section 4. The mixing efficiency of the density field Γ_ρ, equation (2b), deserves some comments. In the absence of DD, heat and salt are mixed at equal rate, $K_h = K_s$, $\gamma = R_\rho^{-1}$, and thus:

$$\begin{aligned} &\textbf{No DD}: \\ &K_\rho = K_{h,s} > 0, \quad P_b = g\alpha_T\overline{w\theta} - g\alpha_S\overline{ws} = -K_\rho N^2 < 0 \end{aligned} \tag{2f}$$

where P_b is the buoyancy production. In this case, *buoyancy acts like a sink*. However, in the presence of DD, at large Ri (small shear) we have for SF $\gamma < 1$, $R_\rho < 1$ while for DC we have $\gamma > 1$, $R_\rho > 1$. In this case we have:

$$\textbf{DD}: \qquad K_\rho < 0, \quad P_b = -K_\rho N^2 > 0 \tag{2g}$$

in which case buoyancy acts like a *source of mixing*.

[6] The heat to salt flux ratio γ exhibits an interesting symmetry. If one exchanges heat with salt $\theta \to s$, $\alpha_T \to -\alpha_s$, one has $R_\rho \Rightarrow R_\rho^{-1}$, $x \Rightarrow -xR_\rho$, and from the first of (2e) it should follow that $K_h \Rightarrow K_s$.This is indeed the case provided:

$$\pi_1 \Rightarrow \pi_4, \quad \pi_3 \Rightarrow \pi_5 \tag{2h}$$

which, given the physical meaning of these variables discussed in section 4, is equivalent to the expected changes $\tau_{ps} \Rightarrow \tau_{p\theta}$, $\tau_s \Rightarrow \tau_\theta$.

3. Dynamical Time Scale τ and the Variable x

[7] Here we discuss how to determine the dynamical time scale τ, equation (2b), or $x = (\tau N)^2(1 - R_\rho)^{-1}$, equation (2e). Consider the production = dissipation relation:

$$\begin{aligned} &P_m + P_b = \varepsilon \quad \Rightarrow \quad K_m\Sigma^2 - K_\rho N^2 = \varepsilon \quad \Rightarrow \\ &Ri^{-1}\Gamma_m - \Gamma_\rho = 1 \end{aligned} \tag{3a}$$

where P_m is the shear production defined as usual as:

$$P_m = -(\overline{uw}U_z + \overline{vw}V_z) = K_m\Sigma^2 \tag{3b}$$

If in the third relation in (3a), which follows from the second using the first of (2b), we substitute (2b, e) and use the dimensionless structure function $S_m(x, Ri, R_\rho)$ given by equation (13a) of C2, we obtain an algebraic relation for x the solution of which is:

$$x = x\left(Ri, R_\rho, \gamma, \pi's\right) \Rightarrow x\left(Ri, R_\rho\right) \tag{3c}$$

The last step comes from the relations for the π's (Ri, R_ρ) derived in the next section.

4. Key New Ingredients: The Relaxation-Dissipation Time Scales

[8] The dynamic equations for the five second-order moments discussed before contain relaxation-dissipation time scales, which in dimensionless form, are called:

$$\pi_1 = \tau_{ps}/\tau, \ \pi_2 = \tau_{s\theta}/\tau, \ \pi_3 = \tau_s/\tau, \ \pi_4 = \tau_{p\theta}/\tau, \pi_5 = \tau_\theta/\tau \tag{4a}$$

which were traditionally [e.g., *Mellor and Yamada*, 1982] assumed constant. An improved set of constants were derived by C2. The C2 values, denoted by a superscript zero, are: $\pi_1^0 = \pi_4^0 = (27Ko^3/5)^{-1/2}(1 + \sigma_t^{-1})^{-1}$, $\pi_3^0 = \pi_5^0 = \sigma_t$, $\pi_2^0 = 1/3$. Here, Ko is the Kolmogorov constant and $\sigma_t = 0.72$ is the (neutral) turbulent Prandtl number. Such relations do not provide a good fit to the variables (1), see Figures 1, 2 and 3 We therefore had to construct a new model in which the π's are functions of the two key variables:

$$\pi_k\left(Ri, R_\rho\right) \tag{4b}$$

The starting point was a recent study [*Canuto et al.*, 2007] (hereinafter referred to as C7) [see also *Zilitinkevich et al.*, 2007] that extended the traditional second-order closure models [e.g., *Cheng et al.*, 2002; C2] to accommodate a new set of DNS (direct numerical simulations), LES (large eddy simulations), lab and field data etc. that showed that mixing persists at almost any Ri dispelling the traditional notion that there exists a critical Ri(cr) above which turbulent mixing essentially vanishes. Specifically, it was shown that the most crucial time scale is $\tau_{p\theta}$ that enters the

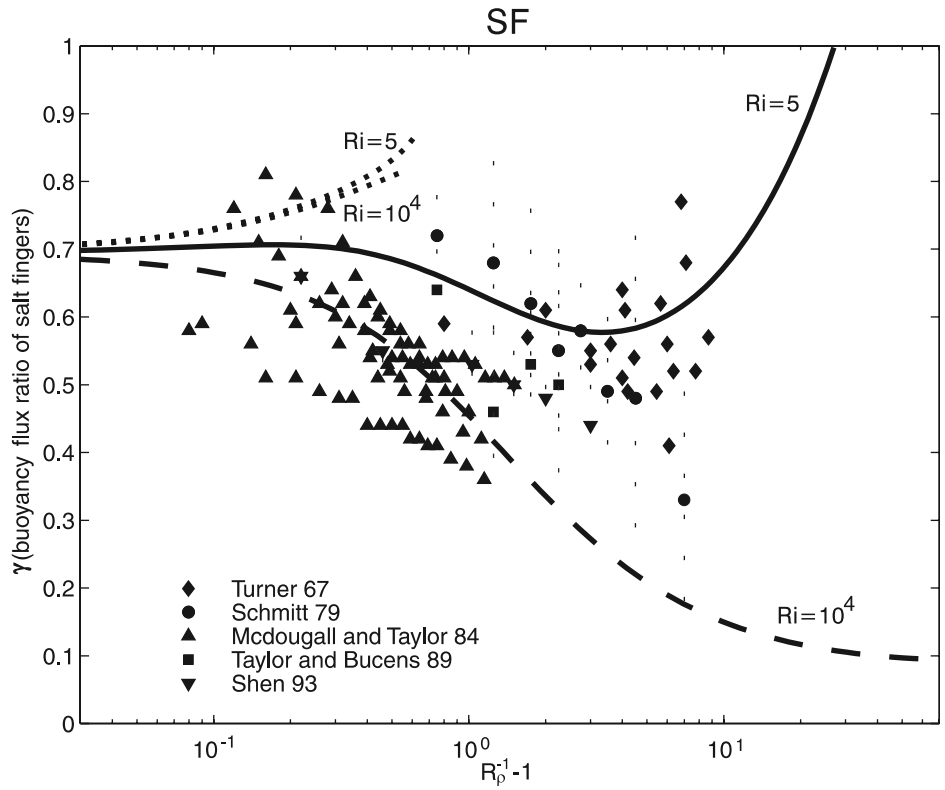

Figure 1. The first function in equation (1) vs. the density ratio for the SF regime. With constant π_k^0, the model results, represented by the short-dashed lines, bunch up in the upper left corner of the figure well outside the bulk of the data [see *St. Laurent and Schmitt*, 1999] and the model becomes unrealizable for $R_\rho < 1/2$. By contrast, the model results using equation (4l), represented by the solid and long-dashed lines, fall within the main range of the data, indicating the importance of the Ri and R_ρ dependence in (4l). For the new model, results for $Ri > 10^4$ are indistinguishable from that of $Ri = 10^4$. Therefore, when DD is active, the model results become Ri independent as $Ri \to \infty$.

heat flux equation. The underlying idea is that stable stratification reduces the heat flux more than the momentum flux [*Gerz et al.*, 1989], thus pointing toward $\tau_{p\theta}$ as a key player. In fact, a dependence on Ri means the interplay between the temperature and velocity fields and the combination most likely to be affected is the heat flux $\overline{w\theta}$ (thus $\tau_{p\theta}$) that entails both those fields. A second reason is the work by *Weinstock* [1978] who showed that stable stratification reduces the time scale by a factor $1 + (\tau N)^2$ which C7 showed to be equivalent to:

$$\tau_{p\theta}/\tau \sim (1 + Ri)^{-1}, \qquad Ri > 0 \tag{4c}$$

To include the effect of both Ri and R_ρ we now suggest to further generalize (4c) to:

$$\tau_{p\theta}/\tau \sim \left[1 + Ri\left(1 + aR_\rho\right)^{-1}\right]^{-1}, R_\rho > 0 \tag{4d}$$

For $R_\rho < 0$, there is no DD tendency and we use (4c). *Why the R_ρ dependence and what is a?* As for R_ρ the rationale is as follows: in the presence of DD, for $R_\rho > 0$, when the salt and temperature gradients act against each other, DD provides a source of mixing in addition to that of shear thus lessening the damping effect of Ri, a fact reflected by the counter factor $(1 + aR_\rho)$. In the limit $R_\rho \gg Ri$, $\pi_4 \sim \pi_4^0$, the effect of Ri on the time scale disappears. As for π_1, its form is derived from (4d) by the symmetry requirement:

$$\tau_{ps} \to \tau_{p\theta} \text{ as } R_\rho \to R_\rho^{-1} \tag{4e}$$

and thus we have:

$$\tau_{ps}/\tau \sim \left[1 + Ri\left(1 + aR_\rho^{-1}\right)^{-1}\right]^{-1} \tag{4f}$$

Note that in the limit of no temperature gradient, $R_\rho = \infty$, $\pi_1 \sim \pi_1^0(1 + Ri)^{-1}$ in analogy with (4c). As for π_2, we suggest a generalization that does not depend on Ri since this time scale represents a correlation between temperature and salinity fields only:

$$\tau_{s\theta}/\tau \sim \left(R_\rho + R_\rho^{-1}\right)^{-1} \tag{4g}$$

because of the following reasons. First, it is the simplest form that satisfies the symmetry requirement

$$\tau_{s\theta} \to \tau_{\theta s} \text{ as } R_\rho \to R_\rho^{-1} \tag{4h}$$

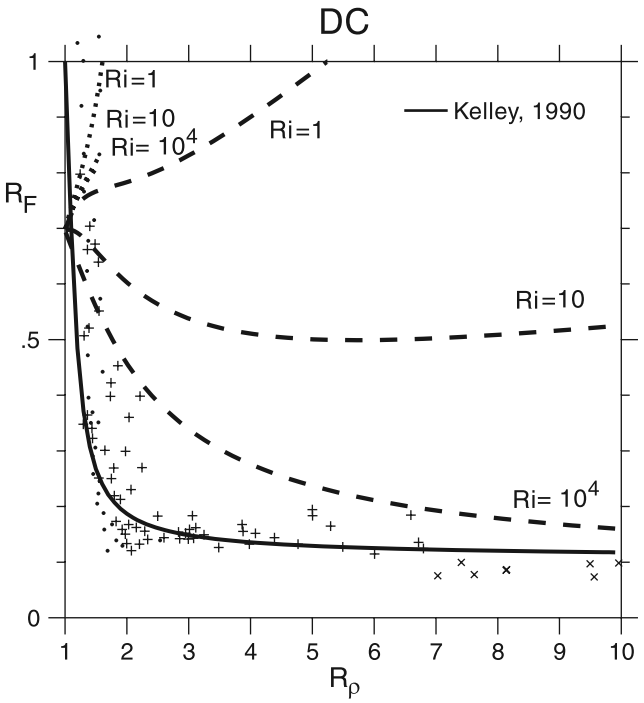

Figure 2. The second function in equation (1) vs. the density ratio for the DC case (dots and crosses are the data from *Kelley* [1990]). The solid line represents the numerical fit by *Kelley* [1990]. As in Figure 1, with constant π_k^0, the model results (short-dashed lines) lump in the upper left corner well outside the bulk of the data. Use of (4l) yields the results represented by long-dashed lines: as expected, the no shear data are best represented by high Ri.

Second, as $R_\rho \sim 0$, $\pi_2 \sim R_\rho \sim 0$ and as $R_\rho \sim \infty$, $\pi_2 \sim R_\rho^{-1} \sim 0$. For the case with tendency to DC ($1 < R_\rho < \infty$), R_ρ^{-1} plays the same role that R_ρ does in the case with tendency to SF ($0 < R_\rho < 1$), when either SF disappears ($R_\rho = 0$) or DC disappears ($R_\rho = \infty$), the salt-heat correlation time scale goes to zero, as these correlations are associated with the double diffusive processes. By heat-salt symmetry, R_ρ and R_ρ^{-1} must appear symmetrically in the salt-heat correlation. Their average, representing double diffusive tendency of either kind, plays a role in the salt-heat correlation somewhat similar to that of stratification in the pressure correlations. *In summary,* $\pi_{1,2,4}$ *were modified as just described while* $\pi_{3,5} = \pi_{3,5}^0$. Finally, we discuss the coefficient a. Consider DC in the limit $Ri \gg 1$ where the data are given in Figure 2. In that limit, the asymptotic values of $\pi_{1,4}$ are:

$$\pi_4 \to a\pi_4^0 R_\rho Ri^{-1}, \quad \pi_1 \to \pi_1^0 Ri^{-1} \tag{4i}$$

It follows that, using (2e), the salt to heat flux ratio R_F becomes:

$$\text{DC}: \qquad R_F = \frac{\alpha_S \overline{ws}}{\alpha_T \overline{w\theta}} \Rightarrow \frac{1}{a}\frac{\pi_1^0}{\pi_4^0} \Rightarrow \frac{1}{a} \tag{4j}$$

Next, using *Linden*'s [1974] result that the asymptotic value of R_F is the square root of the ratio of the salt diffusivity κ_s to the thermal diffusivity κ_T, we obtain:

$$a = (\kappa_T/\kappa_s)^{1/2} \approx 10 \tag{4k}$$

which is the value used in our work. In summary, we now have the new relations:

$$\pi_1 = \pi_1^0\left(1 + \frac{Ri}{1 + aR_\rho^{-1}}\right)^{-1}, \quad \pi_4 = \pi_4^0\left(1 + \frac{Ri}{1 + aR_\rho}\right)^{-1}$$
$$\pi_2 = \pi_2^0\left[\frac{1}{2}\left(R_\rho + R_\rho^{-1}\right)\right]^{-1}, \quad \pi_{3,5} = \pi_{3,5}^0 \tag{4l}$$

which yield the π's in terms of Ri and R_ρ.

5. Full Model

[9] The mixing model is thus complete. First, with the $\pi_k(Ri, R_\rho)$ of (4l) and (3c), one computes γ (Ri, R_ρ), equation (2e). Next, with γ (Ri, R_ρ), π_k (Ri, R_ρ) and x(Ri, R_ρ), from (2b–e) one derives the diffusivities of momentum, heat, salt and density as functions of Ri and R_ρ. Here, we do not need to specify εN^{-2} since we only deal with flux ratios and mixing efficiencies. However, in an OGCM, one must employ the relation:

$$\varepsilon = \varepsilon(\text{ML}) + \varepsilon(\text{igw}) + \varepsilon(\text{tides}) \tag{5}$$

ε(ML) and ε(igw) were discussed in C2, while ε(tides) is given by *Jayne and St. Laurent* [2001].

6. Model Results Vs. Data

[10] In Figure 1 we show the data of heat to salt flux ratio $\gamma(Ri, R_\rho)$ vs. R_ρ for the SF case (see *St. Laurent and Schmitt* [1999] for references on data) on which we have superimposed the model results for Ri = 5, 10^4 for two different models of the π's. In the π_k^0 case, the model's predictions (short-dashed lines), bunch up in the upper left corner outside the bulk of the data. Furthermore, the model becomes unrealizable for $R_\rho \leq 1/2$. With the π's from (4l), the model results (solid and long-dashed lines) reproduce the data for large values of Ri (lab data). Model results for $Ri > 10^4$ are indistinguishable from those at $Ri = 10^4$.

[11] In Figure 2 for DC, we show the salt to heat flux ratio R_F vs. R_ρ, also for the two models of the π's. As in Figure 1, the π_k^0 case yields results (short-dashed lines) that bunch up in the upper left corner outside the bulk of the data and with the incorrect R_ρ dependence. Moreover, the model becomes unrealizable for $R_\rho \geq 2$. Dots and crosses represent the data with no shear by *Kelley* [1990] who also suggested an empirical fitting formula (solid line). With the π's from (4l), the results reproduce the data much better showing the importance of the Ri and R_ρ dependence. As in Figure 1, the model results at high Ri reproduce the no-shear data better.

[12] In Figure 3 we show the heat mixing efficiency $\Gamma_h(Ri, R_\rho)$ using π_k^0. The model results (dashed and full lines) are superimposed on the data from *St. Laurent and Schmitt* [1999]. The model results are acceptable for the strong turbulence case (Ri < 1), panels a)–c), but not as

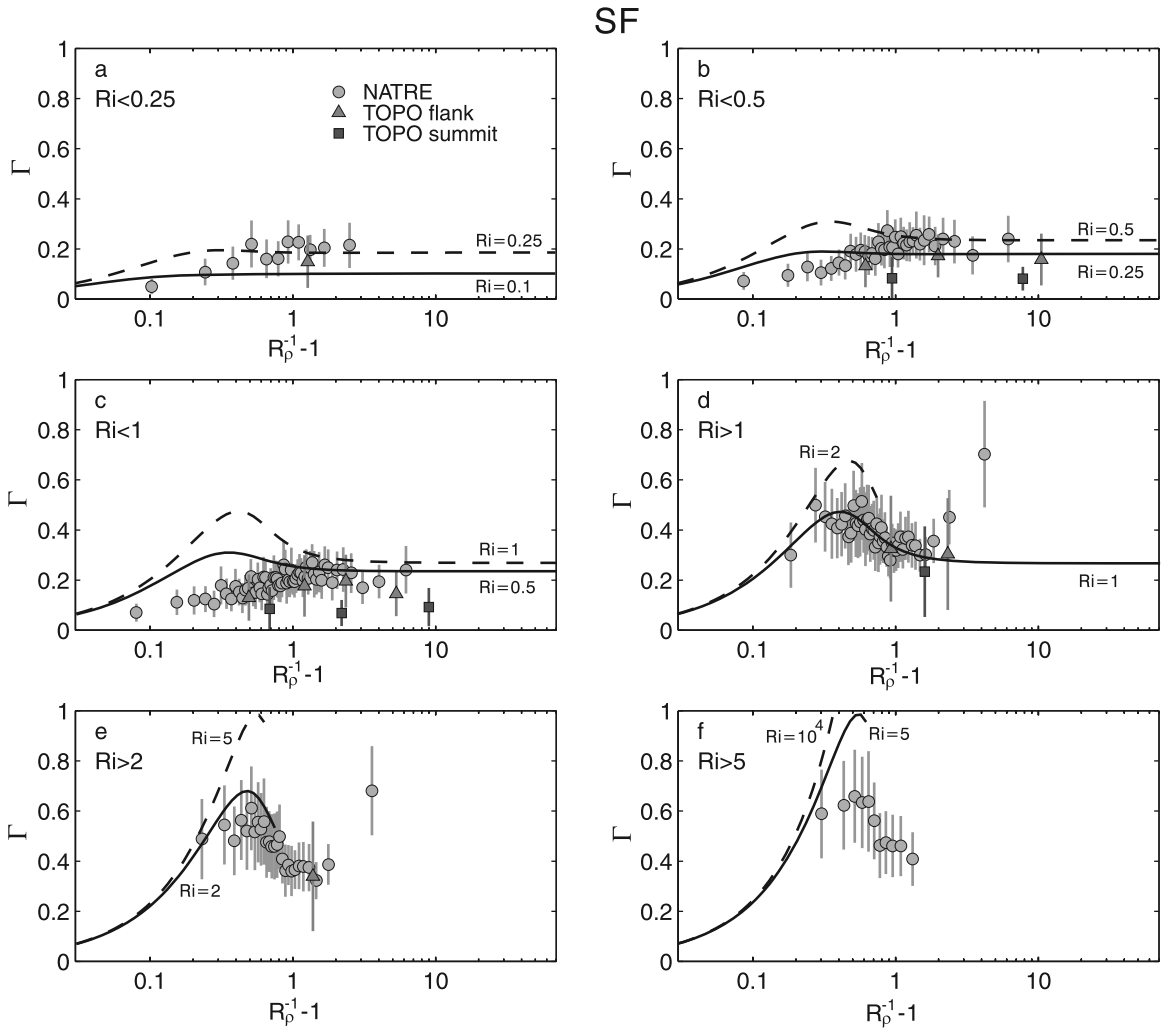

Figure 3. The third function in equation (1), the heat mixing efficiency, for different Ri and R_ρ (data are from *St. Laurent and Schmitt* [1999]). The model results correspond to the π_k^0 and are acceptable for (a, b, c) the strong turbulence case (Ri < 1), but not as good for all the remaining cases.

good for the remaining cases. In Figure 4, we show the heat mixing efficiency Γ_h (Ri, R_ρ) using equation (4l). The model results (dashed and full lines) are superimposed on the same data as in Figure 3. In Figure 4f, the model results for Ri > 10^4 are indistinguishable from those for Ri = 10^4. Use of (4l) considerably improves the model's predictions. As in Figures 1 and 2, as Ri $\rightarrow \infty$, the model results become independent of Ri when DD is active.

7. Conclusions

[13] A model has now been constructed which reproduces reasonably well both laboratory DD data (Ri $\gg$ 1) and ocean data for a range of Ri. The value $\Gamma_h = 0.2$ is now seen to be limited to regions of strong turbulence and no DD, first panel in Figure 3. However, when Ri $\geq$ 1 and turbulence still exists but is weak, DD is active and produces Γ_h's up to three times as large as 0.2, which casts doubts on the computations that employ 0.2 to discuss the "closure of the thermohaline circulation". A map of the density mixing efficiency Γ_ρ showing regions of positive and negative buoyancy, is needed to visualize where DD processes are relevant: if $\Gamma_\rho < 0$, buoyancy acts like a source of mixing whereas in regions where $\Gamma_\rho > 0$ buoyancy acts like a sink, as in ordinary stably stratified flows without DD. As a concrete example, consider the advection-diffusion model where $\overline{w}$ is the diapycnal advection velocity:

$$\overline{w}N^2 = K_\rho \frac{\partial N^2}{\partial z} + N^2 \frac{\partial K_\rho}{\partial z} \tag{6a}$$

Though stratification increases from the bottom up ($\partial N^2/\partial z > 0$), this does not mean that the first term implies *upwelling* $\overline{w} > 0$ since regions of strong DD entail $K_\rho < 0$ and thus the first term can lead to *downwelling* $\overline{w} < 0$. A further important variable is the buoyancy flux integrated over a control volume between two specified density surfaces (TW = terawatts):

$$P_b(TW) = -\int \rho K_\rho N^2 dV = -\int \rho \varepsilon \Gamma_\rho dV \tag{6b}$$

When $P_b > 0$, corresponding to a buoyancy gain, the result can be compared with other *sources of ocean stirring* such

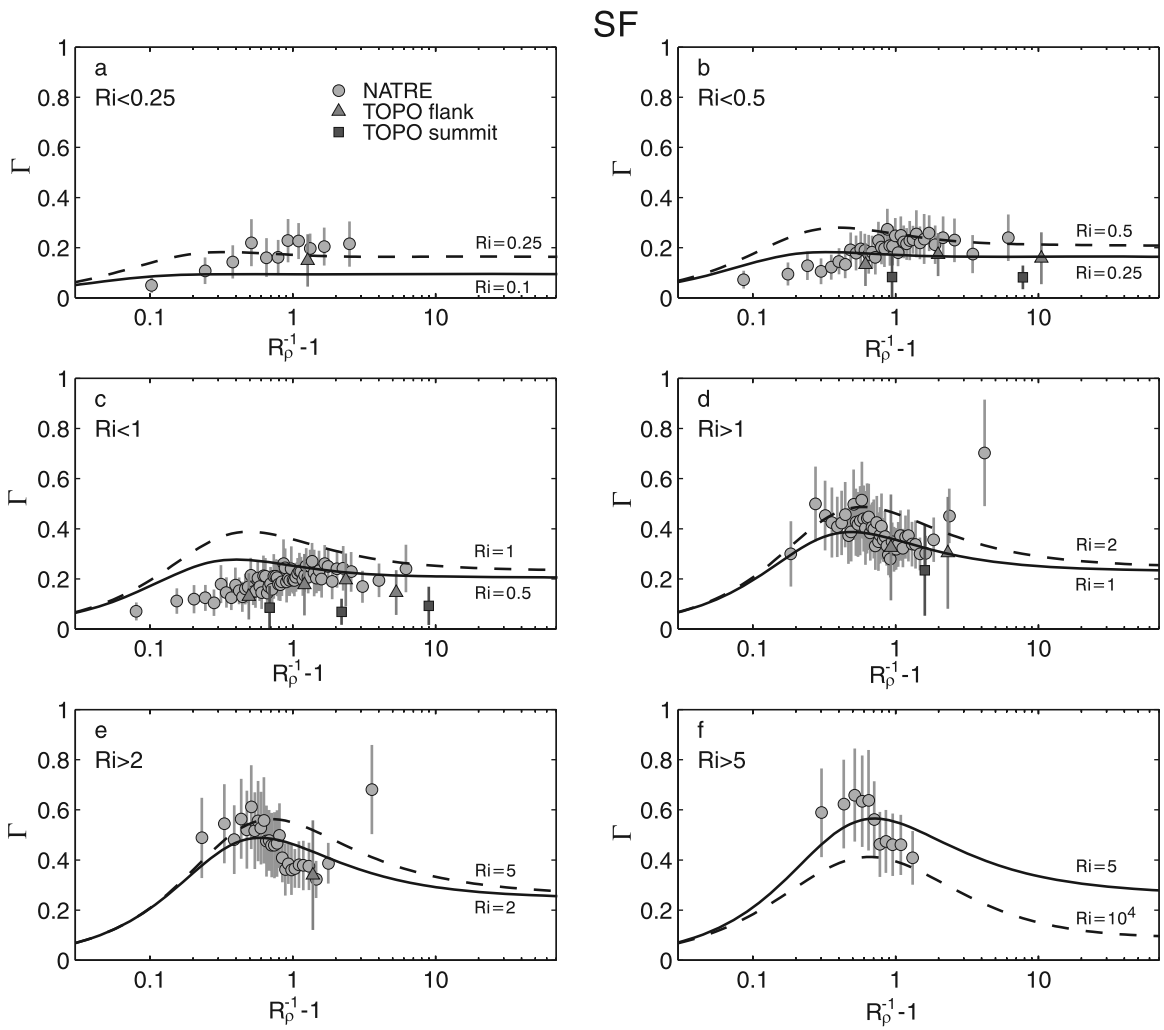

Figure 4. Same data as in Figure 3 but with equation (4l). The model results are consistent with the data at all Ri. (f) The model results for $Ri > 10^4$ are indistinguishable from those for $Ri = 10^4$. As in Figures 1 and 2, the model results become Ri independent as $Ri \rightarrow \infty$ when DD is active.

as wind and tides [*Wunsch*, 2000].With the availability of the new model, these studies are presently being pursued.

[14] **Acknowledgments.** The authors would like to express their thanks to D. E. Kelley, B. R. Ruddick, L. St. Laurent and R. W. Schmitt for their interest in our work as well as to two anonymous Referees for very useful suggestions and criticism.

References

Canuto, V. M., A. Howard, Y. Cheng, and M. S. Dubovikov (2002), Ocean turbulence. Part II: Vertical diffusivities of momentum, heat, salt, mass and passive scalars, *J. Phys. Oceanogr.*, *32*, 240–264.

Canuto, V. M., Y. Cheng, A. Howard, and I. Esau (2007), Stably stratified flows: A model with no Ri(cr), *J. Atmos. Sci.*, in press.

Cheng, Y., V. M. Canuto, and A. M. Howard (2002), An improved model for the turbulent PBL, *J. Atmos. Sci.*, *59*, 1550–1565.

Gerz, T., U. Schumann, and S. E. Elghobashi (1989), Direct numerical simulation of stratified homogeneous turbulent shear flows, *J. Fluid Mech.*, *200*, 563–594.

Hasumi, H., and N. Suginohara (1999), Atlantic deep circulation controlled by heating in the Southern Ocean, *Geophys. Res. Lett.*, *26*, 1873–1876.

Inoue, R., H. Yamakazi, F. Wolk, T. Kono, and J. Yoshida (2007), An estimation of buoyancy flux for a mixture of turbulence and double diffusion, *J. Phys. Oceanogr.*, *37*, 611–624.

Jayne, S. R., and L. C. St. Laurent (2001), Parameterizing tidal dissipation over rough topography, *Geophys. Res. Lett.*, *28*, 811–814.

Kelley, D. E. (1990), Fluxes through diffusive staircases: A new formulation, *J. Geophys. Res.*, *95*, 3365–3371.

Kelley, D. E., H. J. S. Fernando, A. E. Gargett, J. Tanny, and E. Ozsoy (2003), The diffusive regime of double-diffusion convection, *Prog. Oceanogr.*, *56*, 461–481.

Kunze, E. (2003), A review of oceanic salt-fingering theory, *Prog. Oceanogr.*, *56*, 399–417.

Linden, P. F. (1974), A note on the transport across a diffusive interface, *Deep Sea Res. Oceanogr. Abstr.*, *21*, 283–287.

Mellor, G. L., and T. Yamada (1982), Development of a turbulence closure model for geophysical fluid problems, *Rev. Geophys.*, *20*, 851–875.

Muench, R. D., H. J. S. Fernando, and G. R. Stegen (1990), Temperature and salinity staircases in the northern Weddell Sea, *J. Phys. Oceanogr.*, *20*, 295–306.

Ruddick, B., and A. E. Gargett (2003), Oceanic double-diffusion: Introduction, *Prog. Oceanogr.*, *56*, 381–393.

Schmitt, R. W. (1994), Double diffusion in oceanography, *Annu. Rev. Fluid Mech.*, *26*, 255–285.

Schmitt, R. W. (2003), Observational and laboratory insights into salt fingers convection, *Prog. Oceanogr.*, *56*, 419–433.

Smyth, W. D., and S. Kimura (2007), Instability and diapycnal momentum transport in a double diffusive, stratified shear layer, *J. Phys. Oceanogr.*, *37*, 1551–1565.

St. Laurent, L., and R. W. Schmitt (1999), The contribution of salt fingers to vertical mixing in the North Atlantic Tracer Release Experiment, *J. Phys. Oceanogr.*, *29*, 1404–1424.

Walsh, D., and B. Ruddick (2000), Double-Diffusion interleaving in the presence of turbulence: The effect of a non constant flux ratio, *J. Phys. Oceanogr.*, *30*, 2231–2245.

Webb, D. J., and N. Suginohara (2001), Oceanography: Vertical mixing in the ocean, *Nature*, *409*, 37–38.

Weinstock, J. (1978), On the theory of turbulence in the buoyancy subrange of stably stratified flows, *J. Atmos. Sci.*, *35*, 634–649.

Wunsch, C. (2000), Oceanography: Moon, tides and climate, *Nature*, *405*, 743–744.

Zilitinkevich, S. S., T. Elperin, N. Kleeorin, and I. Rogachevskii (2007), Energy- and flux-budget (EFB) turbulence closure model for the stably stratified flows. Part I: Steady-state, homogeneous regimes, *Boundary Layer Meteorol.*, *125*, 167–192, doi:10.1007/s10546-007-9189-2.

V. M. Canuto, Y. Cheng, and A. M. Howard, NASA Goddard Institute for Space Studies, 2880 Broadway, Suite 554, New York, NY 10025, USA. (vcanuto@giss.nasa.gov)